Basic mechanism of grain-boundary internal friction revealed by a coupling model

Y. Shi,[1] W. B. Jiang,[1] Q. P. Kong,[1,*] P. Cui,[1] Q. F. Fang,[1] and M. Winning[2]

[1]*Institute of Solid State Physics, Chinese Academy of Sciences, Hefei 230031, People's Republic of China*
[2]*Institut für Metallkunde und Metallphysik, RWTH Aachen, D-52056 Aachen, Germany*

By taking into account the mutual interaction among relaxation species, the data of grain boundary (GB) internal friction of Al bicrystals obtained in our previous works [Phys. Rev. B **71**, 060101(R) (2005); Phys. Rev. B **72**, 174118 (2005)] are further analyzed based on a coupling model. It is found that the high-angle GBs exhibit a strong coupling; while the low-angle GBs exhibit a weak coupling. It is shown that the basic mechanism of GB internal friction is GB diffusion for high-angle GBs, and dislocation climb for low-angle GBs. The previously puzzling behaviors (measured high activation energy and broad peak width) of GB internal friction in bicrystals with high-angle GBs and in polycrystals are satisfactorily explained in the light of the coupling model.

PACS number(s): 62.40.+i, 61.72.Mm, 61.72.Lk

I. INTRODUCTION

The grain boundary (GB) internal friction peak was discovered 58 years ago and has been extensively investigated in polycrystalline Al and many other materials.[1–9] The peak appears in polycrystals, but disappears in single crystals, indicating that the peak is associated with GBs. It usually exhibits an activation energy higher than that of GB diffusion and a peak width broader than that for single relaxation time. The peak is generally recognized to be induced by anelastic sliding of GBs, but the data of polycrystals involve mixed contributions of different types of GBs, from which the role of an individual GB cannot be evaluated. That is the possible reason that the detailed mechanism of the peak in polycrystals has not been clearly clarified.

In order to reveal the behavior of an individual GB, we investigated the internal friction of Al bicrystals containing tilt GBs with various misorientation angles and tilt axes.[10,11] The bicrystals were made of pure Al with total impurity content 7.7 ppm, the main impurity elements (in ppm) were: P: 3.74, Si: 0.99, Ce: 0.99, Cu: 0.40, and Fe: 0.36, etc. A similar internal friction peak appears in the bicrystals but disappears in the adjoining single crystals, confirming that the peak is associated with GB.

We found that the activation parameters of the peak in the bicrystals are different for low- and high-angle GBs.[10,11] For the low-angle GBs, the activation energies are 1.3–1.4 eV, and the pre-exponential factors of relaxation time are of the order of 10^{-12} s. Such behaviors have been explained by dislocation climb mechanism; i.e., the GB sliding is accomplished by the glide and climb of dislocations composing the GB, and controlled by climb.

However, for the high-angle GBs, the physical meaning of the activation parameters are hardly understood. The measured activation energies are about 1.65 eV for the random and high Σ high-angle GB, as high as 2.0–2.25 eV for the low Σ high-angle GBs, while the pre-exponential factors of relaxation time are several orders smaller than 10^{-12} s. Besides, the peak widths for high-angle GBs are broader than those for low-angle GBs, but narrower than those of polycrystals. Although the measured high activation energies were attributed to the effect of GB structure and impurity segregation,[10,11] the basic mechanism of the peak for high-angle GBs is still not clear.

In the previous investigations in polycrstals and bicrystals, the internal friction was expressed based on the Debye relaxation function, and the peak broadening was attributed to a lognormal (i.e., Gaussian) distribution of relaxation times.[2,8] In the literature up to date, the interaction between basic relaxing species in GB internal friction has not been taken into account.

Although the low-angle GBs can be described by regular arrays of discrete dislocations, the microstructure of high-angle GBs is not fully understood. Nevertheless, any high-angle GB can be considered to include numerous ordered and disordered structural units, and the local concentration of impurities is thought to be higher than the average value owing to impurity segregation.[2,12] We think that in the relaxation process of GBs (especially the high-angle GBs), the correlated motion and mutual interaction between different relaxing species may occur. Hence, the possible role of the coupling effect should be considered.

In the present paper, we attempt to take into account the coupling effect in the GB internal friction to reveal its basic mechanism. It will be seen below that in the light of the coupling model, the previously puzzling problems for polycrystals and bicrystals with high-angle GBs (e.g., measured high activation energy and peak broadening) can be understood, and the basic mechanism emerges.

II. THE COUPLING MODEL

The coupling model proposed by Ngai and co-workers[13–19] is based on the theory of many-body interaction, and has been successfully applied to the relaxation of many correlated systems, such as amorphous polymers, metallic glasses, and glassy ionic conductors. It has also been successfully applied to the correlated relaxation in metals and oxide ceramics, such as the Snoek-Köster relaxation,[20–22] precipitate relaxation,[23] and oxygen ion diffusion.[24] These applications make the basic mechanisms more clearly.

According to this coupling model, the relaxation function $C(t)$ is different in two regions separated by a crossover time t_c. When $t < t_c$, the basic relaxing units relax independently as if the mutual interactions have no effect on the relaxation rate, and the relaxation function takes the form of purely exponential function (the Debye relaxation function)

$$C(t) = \exp(-t/\tau). \tag{1}$$

where τ is the uncoupled (i.e., independent) relaxation time. However, when $t > t_c$, the effects of mutual interactions take hold and slow down the independent relaxation rate, and the relaxation function takes the form of stretched exponential function (a non-Debye relaxation function)

$$C(t) = \exp[-(t/\tau^*)^{1-n}], \tag{2}$$

where τ^* is the coupled (or correlated) relaxation time and n is the coupling parameter with the value of $(0 \leq n < 1)$, which increases as the coupling strength increases.

The existence of t_c is based on theoretical considerations, and confirmed by neutron-scattering experiments and molecular-dynamics simulations. The magnitude of t_c is of the order of 10^{-11}–10^{-12} s for amorphous polymers, and 10^{-12}–10^{-13} s for metals and ionic conductors.[13–19] In internal friction of low-frequencies (~ 1 Hz) as in our case, t_c takes only an insignificant amount of relaxation time, and the relaxation according to Eq. (2) takes practically all the time.

From the condition of continuity of relaxation functions (1) and (2), we have

$$\tau^* = [t_c^{-n}\tau]^{1/(1-n)}. \tag{3}$$

According to Eq. (3) and considering the temperature dependence of relaxation time ($\tau = \tau_0 \exp(E/kT)$, where k is the Boltzmann constant, and T is the absolute temperature), we have

$$E = (1-n)E^*, \tag{4}$$

$$\tau_0 = t_c^n \tau_0^{*(1-n)}, \tag{5}$$

where E and E^* are the uncoupled and coupled activation energies, and τ_0 and τ_0^* are the pre-exponential factors of uncoupled and coupled relaxation times, respectively.

The internal friction can be expressed by the compliances

$$Q^{-1}(\omega) = J_2(\omega)/J_1(\omega), \tag{6}$$

where ω is the circular frequency, J_1 and J_2 are, respectively, the real and imaginary parts of the complex compliance $J(\omega)$, and $J(\omega) = J_1(\omega) - iJ_2(\omega)$. The complex compliance is given by the one-side Fourier transformation of the derivative of the normalized relaxation function $C(t)$, which describes a mechanical relaxation for quasistatic perturbation:

$$J(\omega) = J_U + \delta J \int_0^\infty \left[-\frac{dC(t)}{dt} \right] \exp(i\omega t)dt, \tag{7}$$

where $\delta J = (J_R - J_U)$, J_R is the relaxed compliance, and J_U is the unrelaxed compliance.

Substituting Eq. (2) into (7), we have

$$J_1(\omega) = J_U + (1-n)\delta J \int_0^\infty z^{-n} \exp(-z^{1-n})\cos(\omega\tau^* z)dz, \tag{8}$$

$$J_2(\omega) = (1-n)\delta J \int_0^\infty z^{-n} \exp(-z^{1-n})\sin(\omega\tau^* z)dz, \tag{9}$$

where $z = t/\tau^*$. Using Eqs. (6)–(9), the internal friction as functions of n and $\omega\tau^*$ can be calculated numerically. For the convenience to fit the experimental data, the internal friction can be expressed as functions of n and $\log_{10}\omega$ at constant temperature, or as functions of n and $1/T$ (or $\log_{10}\tau^*$) at constant frequency since $\tau^* = \tau_0^* \exp(E^*/kT)$.[20–23]

When $n = 0$, E^* reduces to E, and the internal friction peak versus $\log_{10}\omega$ or $1/T$ has a symmetrical shape. When $n > 0$, the peak has an asymmetrical shape, the measured E^* and the peak-width increase with the increase of n.[22]

It is noted that there is evidence showing that[25,26] for the coupling strength below a certain threshold, such systems would relax to an uncorrelated state; while for the coupling strength higher than the threshold, the mutual interaction occurs spontaneously. It indicates that when n is below a certain critical value, the relaxation species are essentially independent, and the measured E^* is identical with the uncoupled E.

III. THE APPLICATION TO GB INTERNAL FRICTION

Based on the considerations that the coupling effect (or correlated motion) is possibly involved in the relaxation process of GBs due to their specific microstructures (as mentioned in Sec. I), and that the coupling model is shown to be a useful tool to detect the coupling effect and reveal the basic mechanism of coupled relaxation (as mentioned in the last section), we attempt to apply the coupling model to GB internal friction.

By using a nonlinear fitting procedure, which is established by Wang and Fang based on Eqs. (6)–(9) and has been used for oxygen ion diffusion,[24] we have further analyzed the internal friction data of pure Al bicrystals obtained in Refs. 10 and 11. The net internal friction peak and the background (which is assumed to exponentially increase with temperature) can be resolved from the experimental data, and the value of coupling parameter n at best fit can be concurrently obtained.

Figures 1(a)–1(c) show the examples of $Q^{-1} \sim 1/T$ plots for the pure Al bicrystals with different types of GBs. From the figures, we can see that owing to $n > 0$, the peak shapes are not symmetrical. (If we normalize the net peaks to the same height, we can see clearly that the asymmetry and peak-width increase with the increase of n).

Figure 1(a) shows the case of a low-angle GB with $\langle 100 \rangle$ 7.5°. The coupling parameters of low-angle GBs are $n \leq 0.25$. Figure 1(b) shows the case of a random high-angle GB with $\langle 112 \rangle$ 40.2°. The coupling parameters for the random and high Σ high-angle GBs are in the range of 0.35–0.44.
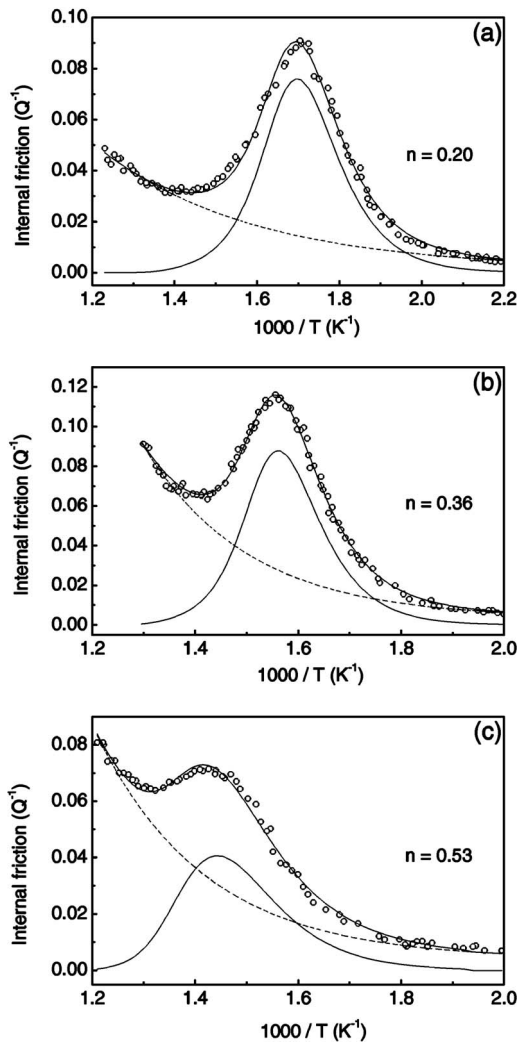
FIG. 1. Internal friction vs reciprocal temperature in pure Al bicrystals with tilt boundaries of (a) $\langle 100 \rangle$ 7.5°, (b) $\langle 112 \rangle$ 40.2°, (c) $\langle 100 \rangle$ 36.0° (close to $\Sigma 5$). The solid line denotes the resolved peak, and the dashed line denotes the background.

TABLE I. The measured activation energy E^*, measured pre-exponential factor of relaxation time τ_0^*, coupling parameter n, decoupled activation energy E, and decoupled pre-exponential factor of relaxation time τ_0 for different misorientation angle θ of $\langle 112 \rangle$ and $\langle 100 \rangle$ tilt boundaries in pure Al bicrystals ($\oplus$ denotes in low-angle region).

Tilt axis	θ	E^* (eV) (± 0.05)	τ_0^* (s)	n (± 0.01)	E (eV) (± 0.05)	τ_0 (s)
$\langle 112 \rangle$	$\oplus 5.8°$	1.39	$10^{-11.3 \pm 1}$	0.22	—	—
	$\oplus 11.1°$	1.44	$10^{-12.2 \pm 1}$	0.25	—	—
	$14.1°$	1.66	$10^{-15.1 \pm 1}$	0.38	1.03	$10^{-13.9 \pm 1}$
	$33.8° \Sigma 35$	1.64	$10^{-14.7 \pm 1}$	0.42	0.95	$10^{-13.6 \pm 1}$
	$40.2°$	1.68	$10^{-14.1 \pm 1}$	0.36	1.08	$10^{-13.3 \pm 1}$
	$44.0° \Sigma 21$	1.65	$10^{-15.4 \pm 1}$	0.44	0.92	$10^{-13.9 \pm 1}$
$\langle 100 \rangle$	$\oplus 7.5°$	1.27	$10^{-11.7 \pm 1}$	0.20	—	—
	$\oplus 9.3°$	1.31	$10^{-11.8 \pm 1}$	0.22	—	—
	$\oplus 14.5°$	1.30	$10^{-11.8 \pm 1}$	0.25	—	—
	$33.4°$	1.99	$10^{-16.3 \pm 1}$	0.49	1.01	$10^{-14.2 \pm 1}$
	$36.0° \Sigma 5$	2.25	$10^{-17.4 \pm 1}$	0.53	1.06	$10^{-14.5 \pm 1}$
	$41.2°$	2.04	$10^{-16.9 \pm 1}$	0.48	1.06	$10^{-14.5 \pm 1}$
	$43.1° \Sigma 29$	1.67	$10^{-15.2 \pm 1}$	0.35	1.09	$10^{-14.1 \pm 1}$

sured data, the activation parameters become more easily to be understood than before. The values of E for low-angle GBs are in the range of 1.3–1.4 eV, which can be attributed to lattice diffusion, while the values of E for high-angle GBs are in the range of 1.0 ± 0.1 eV, which can be attributed to GB diffusion. The detailed analyses will be given in the next section.

The values of τ_0 for low-angle GBs are in the range of $10^{-11} \sim 10^{-12}$ s, which is of the order of the reciprocal of atomic vibration frequency ($1/\nu_D$), while the values of τ_0 for high-angle GBs are in the range of 10^{-13}–10^{-14} s, which is near to but still lower than $1/\nu_D$. The reason for the difference of τ_0 between low- and high-angle GBs is unknown at present.

Figure 1(c) shows the case of a low Σ high-angle GB with $\langle 100 \rangle$ 36.0° (close to $\Sigma 5, 36.9°$), the value of n is as high as 0.53. For the near-low $\Sigma 5$ GBs ($\langle 100 \rangle$ 33.4° and $\langle 100 \rangle$ 41.2°), the values of n are 0.49 and 0.48, respectively.

Table I lists the coupling parameters, measured, and decoupled activation parameters. The measured activation parameters E^* and τ^* are taken from Refs. 10 and 11. The decoupled activation parameters E and τ for high-angle GBs are calculated by using Eqs. (4) and (5) based on the measured E^* and τ^* (which are coupled). In the calculation of τ_0, the crossover time $t_c = 10^{-12}$ s is adopted.

By considering that the coupling parameters of low-angle GBs are below a threshold (see the next section), the measured activation parameters E^* and τ^* are considered as uncoupled.

Figure 2 shows the uncoupled (or decoupled) activation energies E for different misorientation angles in the bicrystals.

We can see from Table I and Fig. 2 that after using the coupling model to exclude the coupling effect from the mea-
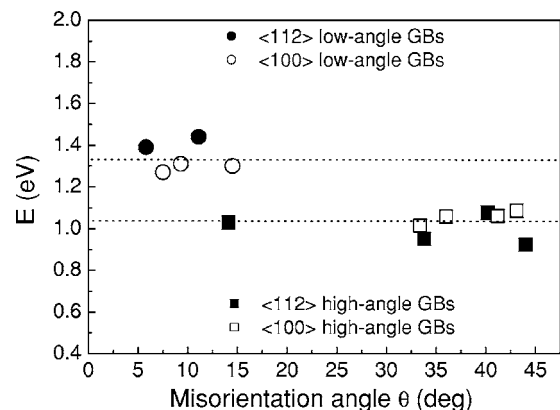

FIG. 2. The uncoupled (or decoupled) activation energy E vs misorientation angle θ for $\langle 112 \rangle$ and $\langle 100 \rangle$ tilt GBs in the bicrystals.

IV. DISCUSSION

The difference in coupling parameters between low-angle GBs ($n \leq 0.25$) and high-angle GBs ($n \geq 0.35$) indicates that a weak coupling occurs for the former, and a strong coupling occurs for latter. The difference of coupling parameters should be associated with the difference of microstructure.

The weak coupling for low-angle GBs might originate from the long-range interaction between the discrete dislocations composing the GB. This viewpoint is supported by the fact that n slightly increases with increasing misorientation angle (Table I). As well known, the spacing d of dislocations composing the low-angle GBs is inversely proportional to the misorientation angle θ,

$$d = b/\theta \qquad (10)$$

where b is the magnitude of Burgers vector. Thus, the increase of θ will lead to a decrease of dislocation spacing and an increase of mutual interaction.

By considering the low coupling parameters ($n \leq 0.25$) and the discrete relaxation units, the coupling strength for low-angle GBs can be considered below the threshold as introduced in Refs. 25 and 26. Here the threshold is thought to be the limit of weak coupling due to long-range interaction; beyond the threshold, the strong coupling due to short-range interaction would occur. Thus, the relaxation species for low-angle GBs can be regarded as independent, and the measured activation parameters for low-angle GBs are actually uncoupled.

The measured activation energies ($E^* = 1.3$–1.4 eV) of low-angle GBs are close to that of lattice self-diffusion (~ 1.3 eV) in Al.[27] By taking into account the possible effect of impurity segregation, the basic mechanism of GB internal friction for low-angle GBs can be attributed to dislocation climb, as suggested in our previous works.

The strong coupling for high-angle GBs ($n \geq 0.35$) might originate from the short-range interaction or correlated motion. In random high-angle GBs, the dislocations will no longer be discrete but possibly degenerate to numerous disordered atom groups. For a relaxation process to occur, an atomic rearrangement in the disordered groups and thus a correlated motion occurs.[2] The high-angle high Σ GBs behave similarly to random high-angle ones,[10,11] and a similar situation is expected.

For the coincidence site lattice (CSL) high-angle GBs (especially the low Σ GBs), the atoms composing the GBs are closely packed and arranged in regular fashion. When an atom moves within the GBs, the adjoining atoms should also adjust their positions to keep the GBs at a low energy state. Accordingly, a strong coupling ($n \approx 0.5$) occurs.

The decoupled activation energies E for the high-angle GBs are found in the same range of 1.0 ± 0.1 eV. It indicates that the basic relaxation processes for the high-angle GBs (including random, high Σ, and low Σ GBs) are the same, but the different coupling strengths result in different measured activation energies E^* for different types of GBs.

Gleiter and Chalmers[9] pointed out that, the activation energies of GB diffusion E_b with respect to that of lattice diffusion E_0 are in the range

$$0.5 E_0 < E_b < 0.8 E_0. \qquad (11)$$

For self-diffusion in Al, E_0 is about 1.3 eV,[27] then E_b for GB self-diffusion is expected in the range of 0.65–1.04 eV. Since the impurities tend to segregate in GBs, the GB diffusion of impurity elements should be involved in GB internal friction. The E_b of impurity GB diffusion is usually higher than that for GB self-diffusion. For example, the E_b of Cu or Fe in Al is about 1.05 eV,[28] which is consistent with the decoupled activation energies (1.0 ± 0.1 eV) for high-angle GBs. Thus, the decoupled activation energies for high-angle GBs in this study can be attributed to GB diffusion (self-GB diffusion combined with impurity GB diffusion, but possibly controlled by the latter).

Based on the coupling model, the peak width should increase with the increase of n, hence the peak widths of high-angle GBs are broader than those of low-angle GBs, as observed.

It seems interesting to compare the uncoupled (or decoupled) activation energies in Fig. 2 with the data of migration. Winning and co-workers[29–32] extensively investigated the unidirectional migration under a constant stress in pure Al bicrystals with $\langle 112 \rangle$ and $\langle 100 \rangle$ tilt GBs. It was observed that the average activation energies of low- and high-angle GBs are respectively close to those of lattice self-diffusion and GB self-diffusion. The dislocation climb was suggested to be the migration mechanism for the low-angle GBs, and GB diffusion was suggested for the high-angle GBs.

Previously, we puzzled over the observations that the measured activation energies of GB internal friction for high-angle GBs are much higher than those of migration. Now it becomes clear that the problem comes from the coupling effect involved in the measured internal friction. After decoupling, we can see that the microscopic mechanism of internal friction is actually the same as that of unidirectional migration. Perhaps because the impurities keep in GBs during internal friction measurement but partly leave off from GBs during long-distance migration, the activation energies of internal friction are slightly higher than those of migration by about 0.15 eV.

So far, we have applied the coupling model to GB internal friction in the bicrystals. Since a polycrystal contains different types of GBs, the GB internal friction of a polycrystal should have a mixed mechanism. Besides, different GBs have different coupling parameters, which will result in a distribution of relaxation times and induce an additional peak-broadening (that is the reason the peak width of a polycrystal is broader than that of a bicrystal). If we simply use the fitting procedure of the coupling model to a polycrystal, the coupling parameter would be overestimated due to the additional peak-broadening.

For example, we have made a trial to apply the coupling model to a pure Al polycrystal (with the same purity as the bicrystals), whose measured activation parameters are $E^* = 1.55$ eV and $\tau_0^* = 10^{-14.4}$ s. Using the abovementioned fitting procedure, we obtain $n = 0.6$, and thus $E = 1.55(1 - 0.6) = 0.62$ eV. Obviously, the coupling parameter n is overestimated and the real activation energy E is underestimated.

Usually a polycrystal has a large fraction of random high-angle GBs. If we adopt the coupling parameter of the random high-angle GBs ($n \approx 0.36$), which is also the mean value of all the bicrystals, to be the overall coupling parameter of the polycrystal, we obtain $E = 1.55(1-0.36) = 0.99$ eV. It is on the same level as that of bicrystals with high-angle GBs. Thus, the behavior of a polycrystal can be represented by that of random high-angle GBs.

In the present paper, we show that the coupling effect is involved in the measured data of GB internal friction, and provide a deeper understanding of the measured data. We think that besides the coupling effect, some other factors (which might interfere in the intrinsic behavior of GB internal friction) should also be considered. As pointed out by Benoit,[6,7] in the case that the GB structure and activation energy are dependent on temperature, the measured activation parameters should be carefully examined.

V. SUMMARY

By taking into account the mutual interaction among relaxation species, we have applied the coupling model to further analyze the GB internal friction of pure Al bicrystals obtained in our previous works, provided a deeper understanding of the measured data, and revealed the basic mechanism of GB internal friction. The main results obtained in the present paper are as follows.

(1) It is found that the coupling parameters are different between low- and high-angle GBs. The low-angle GBs exhibit a weak coupling ($n \leqslant 0.25$), which is attributed to long-range interaction, while the high-angle GBs exhibit a strong coupling ($n \geqslant 0.35$), which is attributed to short-range interaction or correlated relaxation.

(2) By considering that the coupling strength of low-angle GBs is below the threshold, the relaxation species of low-angle GBs can be regarded as uncoupled. Hence, the conclusion deduced from the measured activation parameters is valid, i.e., the basic mechanism of GB internal friction for low-angle GBs is dislocation climb.

(3) The measured high activation energies of high-angle GBs are induced by the coupled relaxation. After "decoupling," the uncoupled activation energies are on the same level as that for GB diffusion. This means that the basic relaxation processes for the high-angle GBs (including random, high Σ, and low Σ GBs) are the same. The basic mechanism of GB internal friction for high-angle GBs is GB diffusion (self-GB diffusion combined with impurity GB diffusion, but possibly controlled by the latter).

(4) The uncoupled (or decoupled) activation energies of low- and high-angle GBs are respectively on the same level as those of unidirectional migration in pure Al bicrystals with $\langle 112 \rangle$ and $\langle 100 \rangle$ tilt GBs. It indicates that the basic mechanisms of GB internal friction and unidirectional migration for the studied tilt GBs are the same.

(5) Since a polycrystal contains different types of GBs, the GB internal friction of a polycrystal has a mixed mechanism. The previously puzzling behaviors (measured high activation energy and broad peak width) of GB internal friction in polycrystals can be explained in the light of the coupling model.

*Author to whom correspondence should be addressed. Email address: qpkong@issp.ac.cn

[1] T. S. Kê, Phys. Rev. **71**, 533 (1947).

[2] T. S. Kê, Metall. Mater. Trans. A **30**, 2267 (1999).

[3] T. S. Kê and P. Cui, Scr. Metall. Mater. **26**, 1487 (1996).

[4] Q. P. Kong, B. Cai, and G. Gottstein, J. Mater. Sci. **36**, 5429 (2001).

[5] Y. Shi, B. Cai, Q. P. Kong, P. Cui, and G. Gottstein, J. Mater. Sci. **38**, 1895 (2003).

[6] W. Benoit, Mater. Sci. Forum **366**, 291 (2001); **366**, 306 (2001).

[7] W. Benoit, Mater. Sci. Eng., A **370**, 12 (2004).

[8] A. S. Nowick and B. S. Berry, *Anelastic Relaxation in Crystalline Solids* (Academic, New York, 1972).

[9] H. Gleiter and B. Chalmers, *High Angle Grain Boundaries* (Pergamon, Oxford, 1972).

[10] Y. Shi, P. Cui, Q. P. Kong, W. B. Jiang, and M. Winning, Phys. Rev. B **71**, 060101(R) (2005).

[11] W. B. Jiang, P. Cui, Q. P. Kong, Y. Shi, and M. Winning, Phys. Rev. B **72**, 174118 (2005).

[12] A. P. Sutton and R. W. Balluffi, *Interfaces in Crystalline Materials* (Oxford University Press, Oxford, 1995).

[13] K. L. Ngai, A. K. Jonscher, and C. T. White, Nature (London) **277**, 185 (1979).

[14] K. L. Ngai and C. T. White, Phys. Rev. B **20**, 2475 (1979).

[15] K. L. Ngai, R. W. Rendell, and H. Jain, Phys. Rev. B **30**, 2133 (1984).

[16] K. L. Ngai and U. Strom, Phys. Rev. B **38**, 10350 (1988).

[17] K. L. Ngai, in *Disordered Effects on Relaxational Properties*, edited by R. Richert and A. Blumen (Springer, Berlin, 1994), pp. 89–150.

[18] K. L. Ngai, Y. N. Wang, and L. B. Magalas, J. Alloys Compd. **211/212**, 327 (1994).

[19] K. L. Ngai and K. Y. Tsang, Phys. Rev. E **60**, 4511 (1999).

[20] Y. Wang, M. Gu, L. H. Sun, and K. L. Ngai, Phys. Rev. B **50**, 3525 (1994).

[21] L. B. Magalas, J. Phys. IV **C8**, 163 (1996).

[22] L. B. Magalas, Solid State Phenom. **89**, 1 (2003).

[23] Y. N. Wang, M. Gu, and L. H. Sun, J. Phys.: Condens. Matter **1**, 10039 (1989).

[24] X. P. Wang and Q. F. Fang, Phys. Rev. B **65**, 064304 (2005).

[25] S. H. Strogatz, R. E. Mirollo, and P. C. Matthews, Phys. Rev. Lett. **68**, 2730 (1992).

[26] K. Y. Tsang and K. L. Ngai, Phys. Rev. E **54**, R3067 (1996).

[27] J. Philibert, *Diffusion et Transport de Matiere dans les Solides* (Les Editions de Physique, Les Ulis Cedex, FR, 1985).

[28] I. Kaur and W. Gust, *Handbook of Grain and Interphase Boundary Diffusion Data* (Ziegler, Stuttgart, 1989).

[29] M. Winning, G. Gottstein, and L. S. Shvindlerman, Acta Mater. **49**, 211 (2001).

[30] M. Winning, G. Gottstein, and L. S. Shvindlerman, Acta Mater. **50**, 353 (2002).

[31] M. Winning, Acta Mater. **51**, 6465 (2003).

[32] M. Winning and A. D. Rollett, Acta Mater. **53**, 2901 (2005).